Metallurgical and Materials Engineering *Research paper*
https://doi.org/10.56801/MME1007

Sorption of Pb^{2+}, Zn^{2+}, Cu^{2+} and Ni^{2+} Ions on Na-enriched Natural Zeolite for Wastewater Treatment Process: A Kinetic Approach

Dragana Radovanović[1], Jelena Dikić[2], Marija Štulović[3], ZoranAnđić[4], Željko Kamberović[5], Sanja Jevtić[6]

[1]*Innovation Center of the Faculty of Technology and Metallurgy in Belgrade Ltd., University of Belgrade, Belgrade, Serbia, divsic@tmf.bg.ac.rs*
[2,3]*Innovation Center of the Faculty of Technology and Metallurgy in Belgrade Ltd., University of Belgrade, Belgrade, Serbia*
[4]*Innovative Centre of the Faculty of Chemistry in Belgrade Ltd., University of Belgrade, Belgrade, Serbia*
[5,6]*Faculty of Technology and Metallurgy, University of Belgrade, Belgrade, Serbia*

Received: 27-07-2023
Accepted: 16-10-2023

Abstract: Low-cost and easily available natural zeolite is a promising adsorbent for metal ions removal in wastewater treatment. The possibility of using zeolitic tuff from Serbia in the form of Na-enriched natural zeolite (Na-Z) for the adsorption of Pb^{2+}, Zn^{2+}, Cu^{2+}, and Ni^{2+} ions from wastewater was investigated in the presented paper. The research included Na-Z characterization and determination of adsorption kinetics in individual ion adsorption tests using Weber-Morris intraparticle diffusion model, non-linear pseudo-first-order (PFO), pseudo-second-order (PSO) and mixed-order (MO) kinetic models. The results indicate that the adsorption processes of metal ions on Na-Z are complex processes dominated by multiple rate-limiting mechanisms and best defined by the MO model. The mechanisms of ion diffusion and adsorption to active sites are equally represented in the Pb^{2+} adsorption process. The mechanism of ion adsorption on the active sites is the rate-limiting step in the Zn^{2+} adsorption process, while in the case of the Cu^{2+} and Ni^{2+} adsorption ion diffusion is the rate-limiting kinetic mechanism. Within the MO model, the PFO rate (external/internal diffusion) and the PSO rate (adsorption on active sites) were calculated and results were applied to a multicomponent wastewater sample in order to determine and explain the adsorption efficiency in wastewater treatment. The results show that the rate of adsorption of individual metal ions and the efficiency of ion removal from a multicomponent wastewater sample are influenced by several factors including the radius of the hydrated ion and the free energy of hydration. The achieved removal of metal ions by Na-Z is Pb^{2+} (89%) > Cu^{2+} (72%) > Zn^{2+} (61%) > Ni^{2+} (58%) and defines Na-enriched natural zeolite as an effective adsorbent in wastewater treatment.

Keywords: Cations; Pseudo-First Order Kinetics; Pseudo-Second Order Kinetics; Mixed-Order Kinetics; Non-Linear Regression; Multicomponent System.

1. Introduction

Rapid population growth and industry development resulted in increased consumption of fresh water and generation of wastewater, as well as the necessity of technologically feasible, eco-friendly, and cost-effective wastewater treatment. European Commission defined chemical precipitation, sedimentation, filtration, flotation, ultrafiltration, activated carbon filtration, and reverse osmosis as the best available techniques for the treatment of wastewater contaminated with heavy metal ions and organics. Disadvantages of these industrially tested and proven methods in wastewater management are high energy consumption, secondary hazardous sludge formation, and operation cost [1]. In contrast to conventional wastewater treatment technologies, adsorption is considered to be an inexpensive and simple technique whose effectiveness depends mainly on the applied adsorbent [2]. In addition to the commonly used adsorbents (activated carbon, clay minerals, polymers, and resins), zeolites are increasingly being investigated and applied in wastewater treatment [3] due to their excellent adsorption and ion exchange properties, high mechanical strength and thermal stability, as well as their low costs [4, 5].

Zeolites are naturally occurring or synthesized alumino-silicate minerals characterized by uniform microporosity and high crystallinity [6]. Zeolites owe specific properties to their three-dimensional TO_4 tetrahedral framework structure (T is Al or Si in a natural zeolite), connected with each other by sharing corner oxygen atoms [7]. The cation exchange capacity of zeolites is based on the partial substitution of Si^{4+} by Al^{3+}, resulting in a negative charge of the framework, balanced by monovalent or divalent cations (Na^+, Ca^{2+}, Mg^{2+} and K^+). These cations are easily exchanged with heavy metal ions from the external liquid medium [8]. Although synthetic zeolites have a higher degree of crystallinity, and thus a higher specific surface area and adsorption efficiency [9], their synthesis involves the use of an organic component as structure directing agent and the generation of waste [10, 11]. For that reason, the easily available and low-cost natural zeolite - clinoptilolite is the most applied zeolite in wastewater treatment [10]. Natural zeolite is usually treated with NaCl solution to ion exchange non-structural ions (Ca^{2+}, Mg^{2+} and K^+) from the alumino-silicate crystal lattice with Na^+ ions from the solution. The ion exchange of these easily mobile cations does not affect the crystallinity of the zeolite, as well as its other physical properties. In the literature, it has been shown that Na-enriched zeolite possesses increased adsorption capacity and rate of heavy metal removal due to the presence of one exchangeable cation in the zeolite structure [10, 12, 13] .

The adsorption of metal ions onto zeolite is an endothermic and spontaneous process [9] and is usually performed in batch and fix-bed systems [10] . Process parameters affecting adsorption efficiency can be divided into (i) system parameters (solid/liquid ratio, pH, temperature, stirring speed, initial concentration of metals in wastewater); (ii) properties of applied adsorbent (chemical and mineralogical composition, specific surface area, diameter and volume of micropores, the average diameter of particles) and (iii) the properties of metal ions (hydrated ion radius, tendency to form hydro-complexes, energy of dehydration) [9, 12]. The mass transfer kinetics of the adsorption process comprises three steps. The first one is the external diffusion of metal ions from the fluid bulk to the adsorbent surface through the liquid film around the adsorbent. The second step is the internal diffusion of metal ions within the pores inside the adsorbent, and the third step is the binding of ions (physical or chemical) to the active sites on both the external and internal surfaces of the adsorbent [14, 15]. One or more of these steps control the rate of the adsorption process and affect the amount of adsorbed metals onto the zeolite [16].

The study of adsorption kinetics is essential for the design and scale-up of adsorption systems. Adsorption kinetics reveals the rate of pollutant removal, the mechanism of the adsorption mass transfer process, and the performance of the applied adsorbent. Several

different kinetic models are applied to determine adsorption kinetics, with pseudo-first-order (PFO) model, pseudo-second-order (PSO) model and Weber-Morris (WM) intraparticle diffusion model being the most frequently used [14, 15, 17, 18]. Due to the complexity of the kinetic models, many authors apply linear regression to solve the PFO and PSO models, and then compare the obtained correlation coefficient (R^2) to determine which model fits better with the experimental results [17, 18]. This procedure leads to a significant error in determining adsorption kinetics because linearization changes dependent/independent variables [14, 15], and PFO and PSO cannot be compared because the units on the ordinates for determining R^2 are different [17]. Lima et al. (2021) [17] compared linearized and non-linearized fitting of both PFO and PSO models for 225 examples of adsorption kinetics found in the literature. The authors showed that, when applying linearized models, the PSO model fits the results better in all 225 cases, while when applying non-linearized models, the PFO model fits better in122 cases (54.2%). For these reasons, it is highly recommended to apply non-linearized forms of the kinetic models in the analysis of adsorption kinetics [14, 15, 17]. Also, PFO and PSO are empirical models and cannot define the mass transfer mechanisms of the adsorption process [9, 14]. Wang and Guo (2020) [14] established the application conditions and the specific theoretical meanings for the PFO and PSO kinetic models. According to these authors, the PFO model may describe the initial stage of adsorption when concentration of adsorbate is very high, a few active sites are occupied and when the (external and internal) diffusion is the rate-limiting mechanism. On the other hand, the PSO model could represent the final stage of adsorption when concentration of adsorbate is low, most of the active sites are occupied and adsorption on active sites could be the rate-limiting step [14].Considering that adsorption is a complex process and may include both the PFO and PSO kinetic processes, Guo and Wang (2019) [18] developed a more general mixed-order (MO) kinetic model in order to describe all conditions and the whole adsorption process. The MO model represents any phase of the adsorption process where diffusion and/or adsorption to active sites can be the rate-limiting mechanism with an arbitrary initial adsorbate concentration in the solution.

The aim of this work is to investigate the kinetics of adsorption and the binding mechanism of various metal cations (Pb^{2+}, Cu^{2+}, Zn^{2+}, and Ni^{2+}) from a monocomponent aqueous solution using Na-enriched natural zeolite from the Zlatokop deposit in Serbia. The obtained results of the kinetic test were applied to a multicomponent synthetic wastewater sample in order to obtain relevant data for the application of this readily available and inexpensive adsorbent for the purification of industrial wastewater.

2. Experimental work

2.1. Modification of natural zeolite

Zeolitic tuff from the Zlatokop deposit (Vranjska Banja, Serbia) was crushed in a ball mill (SFM-1 Desk-Top Planetary Ball Miller, MTI CORPORATION) at a zeolite-ball mass ratio of 1:5 and grinding speed of 250 rpm for 15 minutes, then sieved (Cisa, BA200N, and appropriate sieves) to obtain fraction from 63 to 125 μm. The sample was rinsed with deionized water to remove surface impurities. The modification was performed by mixing 20.0 g of zeolite tuff with 1.0 dm^3 of a 2 M NaCl solution (sodium chloride, Fisher Chemicals, p.a.). The suspension was mixed on a magnetic stirrer (RCT basic IKA MAG) at a temperature of 70 °C and a speed of 400 rpm for 24 h. The solid fraction was filtered and washed with deionized water until negative reaction for chloride ions and dried at 80 °C for 24 h.

2.2. Characterization of natural zeolite and Na-enriched natural zeolite

The cation exchange capacity (CEC) value of natural zeolite was determined by suspending a 1.0 g of zeolite sample in 100 cm^3 of a 1 M CH_3COONH_4 solution (ammonium acetate, Sigma Aldrich, p.a). The suspension was mixed in a water bath at a speed of 105 rpm at 25 °C for 24 h. Separation of the suspension was performed by filtering through filter paper of medium porosity, using a vacuum pump. The concentration of Na^+, Ca^{2+}, K^+ and Mg^{2+} in the solution was determined by atomic adsorption spectrophotometry (AAS) using a Varian Spectra AA 55B device. The CEC value was calculated by adding the concentrations of alkaline and alkaline earth ions in the solution and expressed in mmol M^+/100 g.
The properties of Na-enriched zeolite (Na-Z) were determined using the following analyses. The identification of the phases present in the sample was carried out by the X-ray powder diffraction (XRPD) method. An Ital Structures APD2000 diffractometer was used. The intensities of the diffracted X-ray radiation were measured by CuKα radiation (1.54184 Å) at room temperature in the 2Θ interval of 5-40°, with a step of 0.02° and a hold of 0.5 s. The thermal properties were examined by thermogravimetric analysis (TG-DTA) by heating in a stream of N_2 gas at a flow rate of 100 $cm^3 \cdot min^{-1}$) and a heating rate of 20 °C·min^{-1} up to a temperature of 800 °C. The SDT Q600 instrument, TA Instruments, was used. The specific surface area of the samples was determined by the BET method (Brunauer, Emmett, and Teller) using the Micromeritics ASAP 2020 device. The morphology was examined by scanning electron microscopy (SEM) (SUPRA 35 VP, Carl Zeiss, and FE-SEM TESCAN MIRA 3 XMU). The elemental composition was determined by energy dispersive spectrometry (EDS) (Oxford Inca 3.2 connected to SEM Jeol JSM 5800, at an operating voltage of 20 keV).

2.3. Adsorption kinetics of Pb^{2+}, Cu^{2+}, Ni^{2+} and Zn^{2+} ions on Na-enriched natural zeolite

Aqueous solutions of individual metals of defined concentration were obtained by adding a certain mass of appropriate metal salts to 1.0 dm^3 of deionized water, as listed in Table 1.

Table 1. *Mass of metal salts for aqueous solutions of appropriate concentrations*

Metal	Metal salts, p.a.	Manufacturer	Mass, g	Concentration, mg·dm^{-3}
Zn	$Zn(CH_3COO)_2 \cdot 2H_2O$	Zorka	0.168	50
Pb	$Pb(NO_3)_2$	Fisher Chemicals	0.077	50
Cu	$CuSO_4 \cdot 5H_2O$	Zorka	0.126	50
Ni	$NiSO_4 \cdot 7H_2O$	Fluka	0.239	50

Adsorption kinetics was investigated by adding 1.0 g of Na-Z sample to 100 cm^3 of each metal solution, liquid to solid ratio (L/S) of 100 $cm^3 \cdot g^{-1}$. The suspensions were allowed to stir continuously in a water bath (Memmert, WPE 45) at 25 °C for 24 h at a constant speed of 105 rpm. After a certain time (0.5; 1; 2; 4; 6 and 24 h), aliquots of the solution (2.0 cm^3) were taken for analysis and filtered through a membrane filter (pore diameter 0.45 μm). The concentration of metals in the filtrate was determined by AAS. Tests were performed in triplicate for each metal. The amount of adsorbed metal at a certain time (qt, mg·g^{-1}) was calculated using Equation 1:

$$q_t = \frac{C_0 - C_t}{m} \cdot V \quad (1)$$

where C_0 is the initial concentration, C_t is the concentration after time t, V is the volume of the sample and m is the mass of the adsorbent.

In this work the Weber-Morris (WM) intraparticle diffusion model, non-linear pseudo-first-order (PFO), pseudo-second-order (PSO) and mixed-order (MO) kinetic models were applied to investigate the adsorption kinetics of metal ions onto Na-Z. The WM model equation can be written as Equation (2):

$$q_t = k_{ip} t^{0.5} + I_i \tag{2}$$

where qt is the adsorption capacity ($mg \cdot g^{-1}$) at time t (min), k_{ip}, the slope from the plot of qt versus $t^{0.5}$, is the intraparticle diffusion rate constant ($mg \cdot g^{-1} \cdot min^{-0.5}$); and I_i is the intercept that is proportional to the boundary layer thickness ($mg \cdot g^{-1}$).

The PFO, PSO and MO models can be presented as differential Equations 3, 4 and 5, respectively:

$$\frac{dq_t}{dt} = k_1 \left(q_e - q_t \right) \tag{3}$$

$$\frac{dq_t}{dt} = k_2 \left(q_e - q_t \right)^2 \tag{4}$$

$$\frac{dq_t}{dt} = k_1' \left(q_e - q_t \right) + k_2' \left(q_e - q_t \right)^2 \tag{5}$$

In which q_e ($mg \cdot g^{-1}$) is the experimental equilibrium adsorption amount, k_1 (min^{-1}) and k_2 ($g \cdot mg^{-1} \cdot min^{-1}$) are the PFO and PSO rate constants, respectively. The models were solved using user interface based on Excel software and provided by Wang and Guo (2020) [14], and correlation coefficient (R^2) was used to assess the fitting results and to compare applied models. Within MO model the PFO and PSO rate ($mg \cdot g^{-1} \cdot min^{-1}$) was calculated by Equations 6 and 7, respectively:

$$PFO\ rate = k_1' \left(q_e - q_t \right) \tag{6}$$

$$PSO\ rate = k_2' \left(q_e - q_t \right)^2 \tag{7}$$

2.4. Wastewater treatment

The results obtained by adsorption kinetics research were applied to a synthetic wastewater sample. The wastewater sample was made by adding defined amounts of metal salts to 1.0 dm^3 of deionized water to obtain metal concentrations according to Table 1. The 3 samples of 100 cm^3 were taken from the multicomponent synthetic wastewater solution and 10.0 g of Na-Z was added to each sample (L/S of 10 $cm^3 \cdot g^{-1}$). The increase in the mass of zeolite, i.e., the reduction of the L/S ratio from 100 to 10 $cm^3 \cdot g^{-1}$ in the wastewater treatment test, was aimed at increasing the available surface of the adsorbent and the number of active sites for adsorption, based on the results obtained in the adsorption kinetics tests. The suspensions were treated and the adsorption process was further investigated in the same way as described in chapter 2.3. The applied adsorption process for the removal of the metal ions from the wastewater sample was evaluated by calculating the amount of adsorbed ions over time (qt) according to Equation 1, and the process efficiency (Ef., %) was determined using Equation 8.

$$Ef = \frac{C_0 - C_t}{C_0} \cdot 100\% \quad (8)$$

3. Results and discussion

3.1. Results of Na-enriched natural zeolite characterization

Figure 1a shows the powder diffraction pattern of the Na-Z sample. The peaks at 2Θ(°) positions: 9.7; 12.8; 17.2; 19; 22.2 and 29.9 can be attributed to clinoptilolite [19]. Feldspar, quartz and clay phases are also present in the zeolite tuff as impurities. Figure 1b shows the TG and DTG curves of the Na-Z sample. The observed total mass loss of about 10 wt.%. is caused by dehydration. The maxima on the DTG curve are located at temperatures of 91, 343, 467 and 671 °C, so it was concluded that dehydration takes place in four steps. The maximum at 91 °C can be attributed to the evaporation of surface-bound water, while at higher temperatures there is a loss of water molecules from the channels and cavities of the zeolite lattice.
The specific surface area of the natural zeolite sample from the Zlatokop deposit and Na-enriched zeolit, calculated on the basis of BET analysis, were 38 and 41 m^2g^{-1}, respectively, which corresponds to previously published results [20] . Usually, the volume of micropores in this type of natural zeolite ranges from 0.003 to 0.005 cm^3g^{-1}, while the specific surface is in the range of 15-40 m^2g^{-1} [20]. The cation exchange capacity (CEC) of natural zeolite, determined based on the concentration of Na, Ca, K and Mg in the solution, is 176 mmol M^+ per 100 g of zeolite. Micrographs of the Na-Z sample presented in Figure 2 show that the structure of the particles is non-uniform, irregularly shaped and that the particles are grouped into aggregates up to 50 μm in size. The results of the elemental EDS analysis confirm the aluminate-silicate nature of Na-Z with a dominant content of Si (22.3 at.%), O (69.4 at.%) and Al (4.6 at.%). The content of Na (3.2 at.%) is significantly higher than Mg (0.2 at.%), K (0.2 at.%) and Ca (0.1 at.%) content due to the Na-modification of natural zeolite.

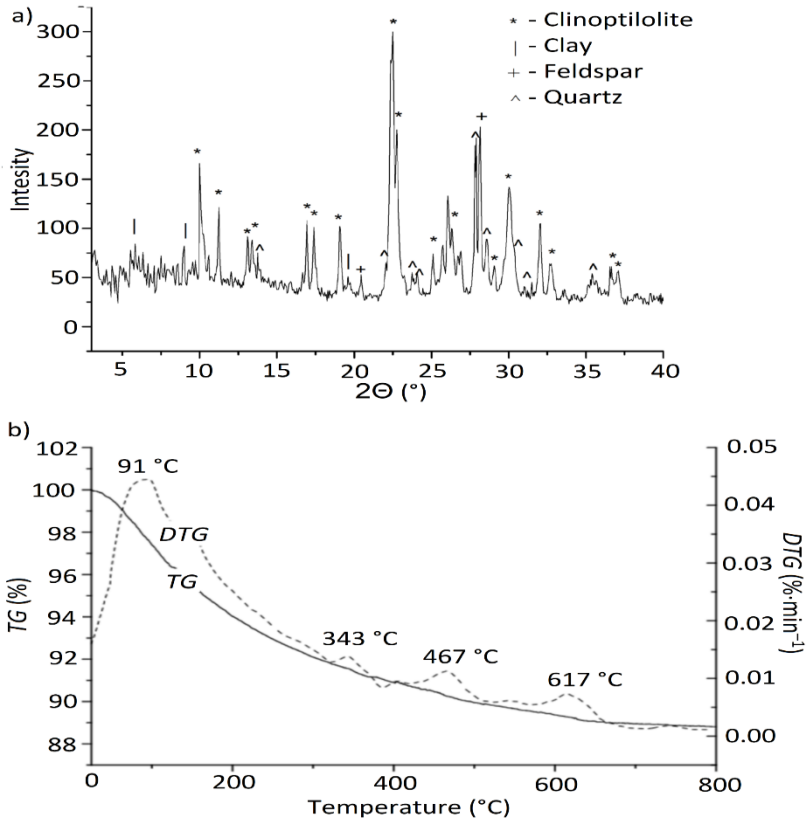

Figure 1. *a) Powder diffractogram and b) TG and DTG curves of Na-enriched natural zeolite*

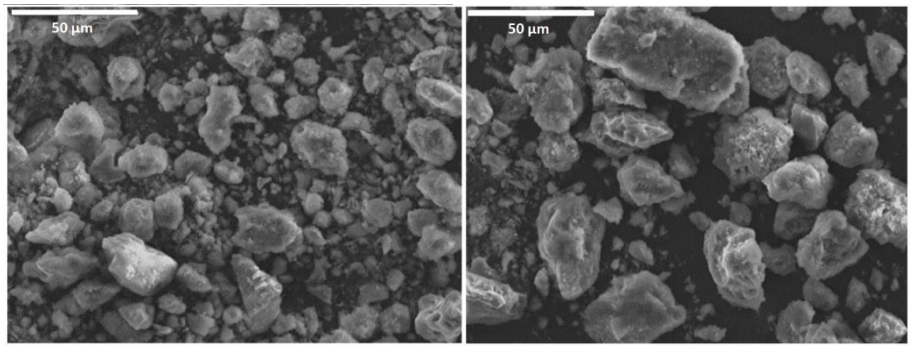

Figure 2. *Micrographs of the Na-enriched natural zeolite sample*

3.2. Adsorption kinetics

The WM intra-particle diffusion model was applied to provide an understanding of the adsorption mechanism and to examine whether the diffusion process through the particle (internal diffusion) is the rate-limiting step [21]. The WM model is solved by plotting the *qt* values versus the $t^{0.5}$ values to determine the model parameters k_{ip} as the slope of the straight line and I_i as the intercept on the y-axis. The WM model plots gained for Pb^{2+}, Zn^{2+}, Cu^{2+} and Ni^{2+} ions are presented in Figure 3, and model parameters in Table 2.

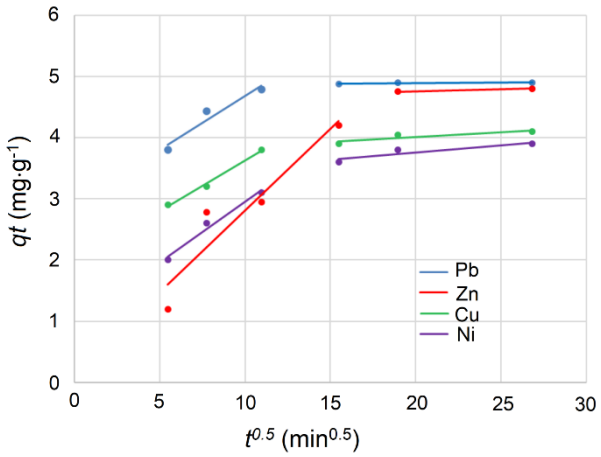

Figure 3. *Weber-Morris plots for the adsorption of Pb^{2+}, Zn^{2+}, Cu^{2+} and Ni^{2+} using Na-Z*

Table 2. *Weber-Morris model parameters for the adsorption of Pb^{2+}, Zn^{2+}, Cu^{2+} and Ni^{2+} using Na-Z*

Parameter	Pb		Zn		Cu		Ni	
	1. line	2. line	1. line	2. line	1. line	2. line	1. line	2. line
k_{ip}, mg·g^{-1}·min$^{-0.5}$	0.1762	0.0015	0.2670	0.0064	0.1658	0.0159	0.1978	0.0241
I_i, mg·g^{-1}	2.9200	4.8634	0.1345	4.6293	1.9636	3.6877	0.9722	3.6877
R^2	0.9364	0.5425	0.8882	1.0000	0.9917	0.8138	0.9773	0.8138

As shown in Figure 3, all studied ion concentrations did not yield a straight line passing through the origin (0,0). This indicates that the adsorption of Pb^{2+}, Zn^{2+}, Cu^{2+} and Ni^{2+} using Na-Z is a complex process and that intraparticle diffusion is not the sole rate-limiting step in the adsorption mechanism [14, 21, 22]. The kinetic plots are presented as two linear lines for each investigated ion. The bilinear graphs describe the gradual increase of adsorption capacity and then its flattening as the process reaches equilibrium, which denotes the occurrence of two steps involved in the adsorption process. The first step is rapid ($k_{ip}1 > k_{ip}2$ for all investigated ions) and represents mass transfer through the liquid film around the Na-Z particle (external diffusion) attributed to the availability of more empty sites at the beginning of the adsorption process. The second step represents ions diffusion into the internal pore structures of Na-Z and is shown as almost horizontal lines due to the decrease of free active sites indicating the saturation of the adsorbent [21-24]. Also, it can be seen that I_i, as the boundary layer thickness, is greater in the second step ($I_i2 > I_i1$ for all investigated ions) denoting its enhanced effect in the later part of the adsorption process [22].

Experimental data obtained in adsorption tests of individual metals ion were then fitted using the PFO, PSO and MO kinetic models and the results are shown in Figure 4 for Pb^{2+} and Zn^{2+} ions, and in Figure 5 for Cu^{2+} and Ni^{2+} ions. In addition, the kinetic and statistical parameters calculated from the non-linear forms of the kinetic models are shown in Table 3 for their comparison.

Table 3. *Adsorption kinetics and statistical parameters of PFO, PSO and MO kinetic model*

Model	Parameters	Pb^{2+}	Zn^{2+}	Cu^{2+}	Ni^{2+}
Experimental	q_e, mg·g^{-1}	4.90	4.85	4.10	3.90
PFO	k_1, min^{-1}	0.0487	0.0102	0.0380	0.0211
	R^2	0.9980	0.9749	0.9839	0.9813
	q_e, mg·g^{-1}	4.85	4.79	3.94	3.70
PSO	k_2, mg·g^{-1}·min^{-1}	0.0216	0.0021	0.0166	0.0073
	R^2	0.9987	0.9720	0.9967	0.9984
	q_e, mg·g^{-1}	5.05	5.61	4.17	4.08
MO	k_1', min^{-1}	0.0192	0.0063	0.0027	0.0034
	k_2', mg·g^{-1}·min^{-1}	0.0134	0.0013	0.0165	0.0071
	R^2	0.9999	0.9754	0.9967	0.9985
	q_e, mg·g^{-1}	4.90	4.82	4.07	3.86

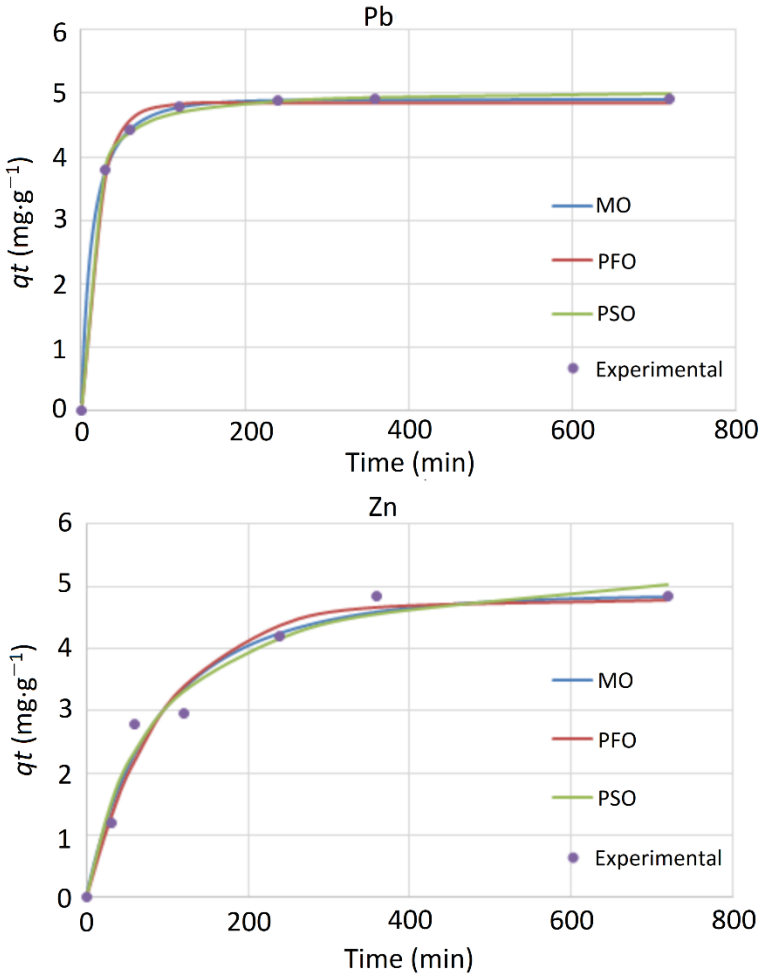

Figure 4. *Adsorption kinetics data of Pb^{2+} and Zn^{2+} ions on Na-enriched natural zeolite fitted by PFO, PSO and MO kinetic model*

By interpreting the results shown in Figures 4 and 5 and Table 3, it can be seen that all three models have excellent results in fitting the experimental data (values of the statistical parameter $R^2 > 0.97$). However, the MO model showed the best-fitting results for all investigated metal ions compared to the other two models which is also reflected in the values of q_e obtained by modeling and determined experimentally. The values of q_e calculated by the MO model are significantly closer to the experimental ones than the values obtained using the PFO and PSO models. The values of pseudo-first-order rate constant (k_1') and pseudo-second-order rate constant (k_2') within the MO model >0 indicate that adsorption processes of metal ions are the combination of the PFO and PSO kinetic processes and that the processes are dominated by multiple rate-limiting steps [18]. The close values of R^2 for the PFO and PSO models in the case of adsorption of Pb^{2+} (0.9980 and 0.9987) and Zn^{2+} ions (0.9749 and 0.9720) demonstrate the complexity of their adsorption process, which is best described by more general form such as the MO model (R^2 values of 0.9999 and 0.9754 for Pb^{2+} and Zn^{2+} adsorption process respectively). The complexity of the adsorption process of Pb^{2+} and Zn^{2+} ions is also reflected in the values of the rate constants for the PFO and PSO models, k_1 and k_2, respectively, as well as in the values of k_1' and k_2' calculated for the MO model. For the adsorption of Pb^{2+} ions, k_1 and k_2 are of the same order of magnitude (0.0487 min^{-1} and 0.0216 $mg \cdot g^{-1} \cdot min^{-1}$), and k_1' (0.0192 min^{-1}) and k_2' (0.0134 $mg \cdot g^{-1} \cdot min^{-1}$) are very close, indicating that both mechanisms of ion diffusion and adsorption to active sites could be rate-limiting in this process. In the case of Zn^{2+} ion adsorption, the situation is somewhat different. The value of k_1 (0.0102 min^{-1}) is an order of magnitude higher than k_2 (0.0021 $mg \cdot g^{-1} \cdot min^{-1}$), and k_1' (0.0063 min^{-1}) is higher than

k_2' (0.0013 mg·g^{-1}·min^{-1}). Although the kinetics of the process can be well described by both the PFO model (R^2=0.9749) and the PSO model (R^2=0.9720), the process of ion diffusion occurs more rapidly than adsorption to active sites indicating that adsorption on active sites is the rate-limiting mechanism of Zn^{2+} ion adsorption.

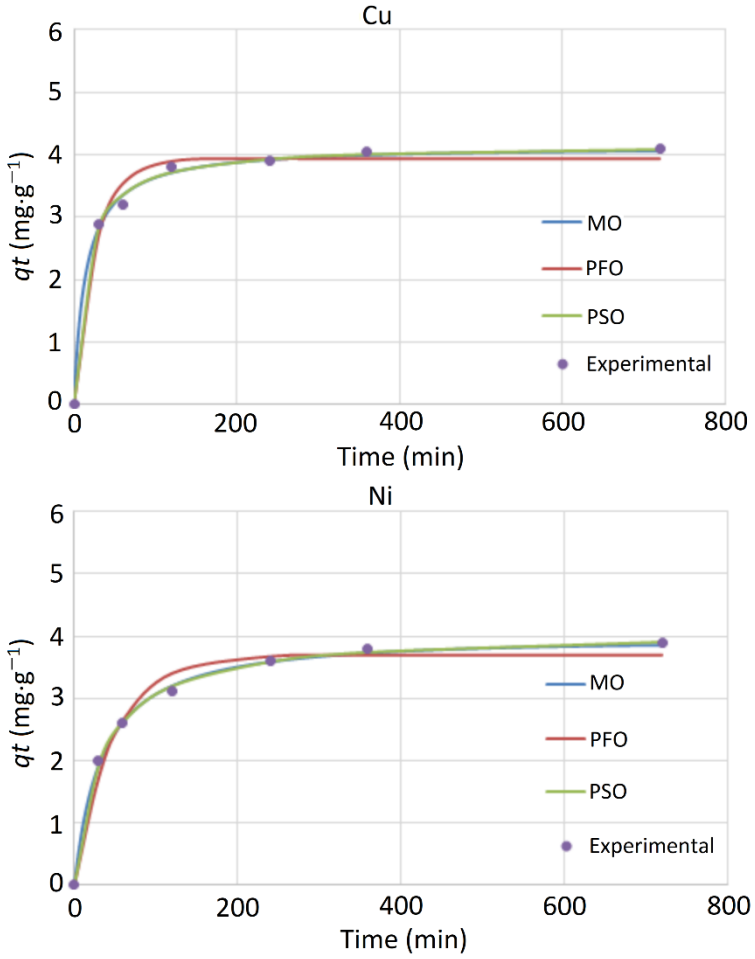

Figure 5. *Adsorption kinetics data of Cu^{2+} and Ni^{2+} ions on Na-enriched natural zeolite fitted by PFO, PSO and MO kinetic model*

In the case of the adsorption of Cu^{2+} and Ni^{2+} ions, the R^2 value for the PSO model (0.9967 and 0.9984, respectively) is higher than for the PFO model (0.9839 and 0.9813, respectively) and almost the same as the R^2 value for the MO model (0.9967 and 0.9985, respectively). Also, k_2' values (0.0165 mg·g^{-1}·min^{-1} for Cu^{2+} and 0.0071 mg·g^{-1}·min^{-1} for Ni^{2+}) are significantly higher than k_1' (0.0027 min^{-1} for Cu^{2+} and 0.0034 min^{-1} for Ni^{2+}) and almost the same as k_2 values (0.0166 and 0.0073 mg·g^{-1}·min^{-1}, respectively). This indicates that PSO kinetics (adsorption on the active sites) is the rapid mechanism in this adsorption process, which means that the ion diffusion could be addressed as the rate-limiting mechanism of Cu^{2+} and Ni^{2+} ions adsorption. The rate of overall adsorption kinetics (PFO and PSO adsorption rate) within the MO kinetic model were calculated based on Equations 6 and 7, and results are shown in Figure 6 for Pb^{2+} and Zn^{2+} ions, and in Figure 7 for Cu^{2+} and Ni^{2+} ions.

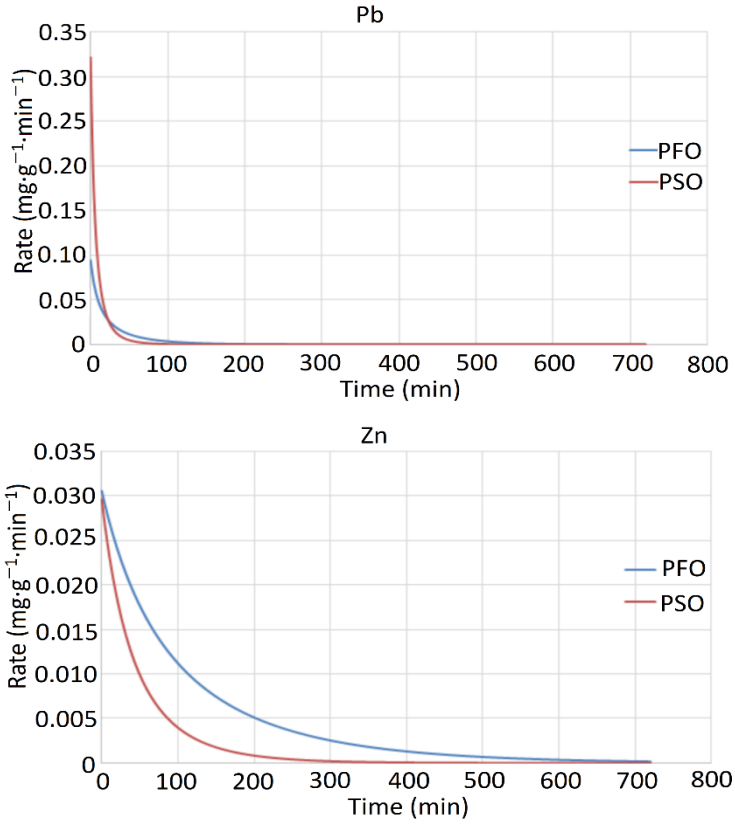

Figure 6. *Adsorption rate of Pb^{2+} and Zn^{2+} ions on Na-enriched natural zeolite according to the MO kinetic model*

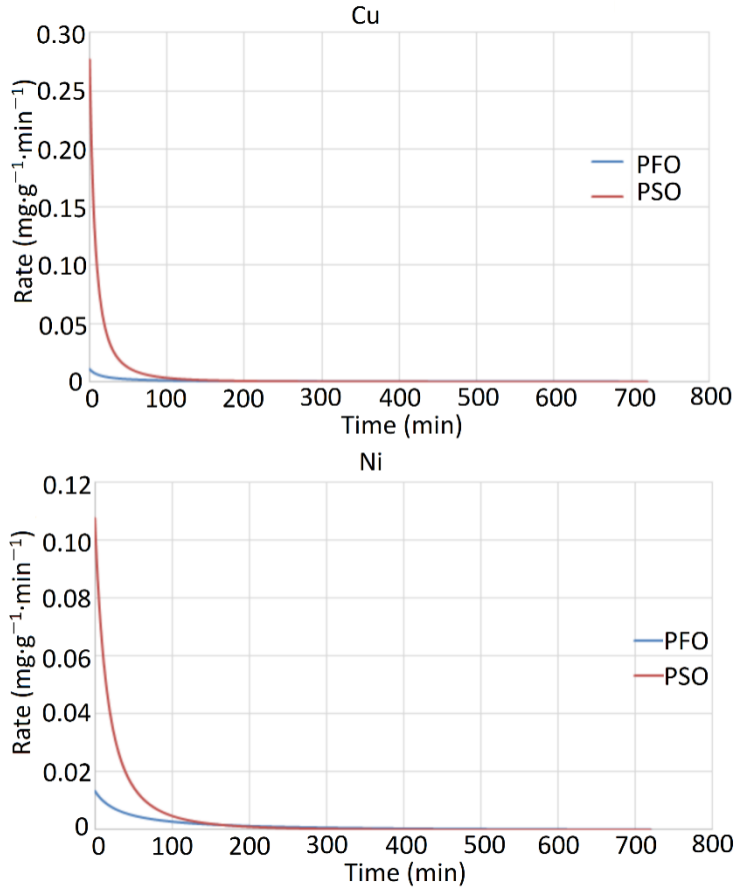

Figure 7. *Adsorption rate of Cu^{2+} and Ni^{2+} ions on Na-enriched natural zeolite according to the MO kinetic model*

In the case of Cu^{2+} and Ni^{2+} ions adsorption, it can be seen that the PSO rate (the rate of adsorption on the active sites) is an order of magnitude higher than the PFO rate (the rate of mass transfer processes – external and internal diffusion), Figure 7. This confirms that the adsorption on the active sites is the rapid kinetic process, while diffusion of ions is the rate limiting step for Cu^{2+} and Ni^{2+} adsorption. The rapid kinetic of adsorption on active sites for Cu^{2+} ions can be explained by the Jahn-Teller effect and easy complexation characteristic for Cu^{2+} ions [25], while Khan et al. (2021) [26] confirmed that potential of Ni^{2+} adsorption onto zeolite is proportional to the number of available active sites. The same order of magnitude of the PFO and PSO rates in the case of Pb^{2+} and Zn^{2+} ions adsorption (Figure 5) confirms that multiple mechanisms dominate this process. Figures 6 and 7 also show that the adsorption rates are highest at the beginning of the process and, for Pb^{2+}, Cu^{2+}, and Ni^{2+} ions, decrease dramatically until a quickly established equilibrium, which is before 100 min for Pb^{2+} and Cu^{2+} ions, and around 150 min of the process time for Ni^{2+} ions. The PFO and PSO rates of the Zn^{2+} ions adsorption process are of the same order of magnitude as the PSO rate of Ni^{2+}ions, however, the adsorption equilibrium is reached much later, after 600 minutes of the process. Guo and Wang (2019) [18] stated that modification of the adsorbate to increase the amount of the active sites may improve the PSO adsorption kinetics. On the other hand, the adsorption process controlled by the external/internal mass transfer (PFO kinetics) may be improved by increasing of specific surface and pore volumes of the adsorbate. Therefore, in the following adsorption tests for the removal of metal ions from a multicomponent synthetic wastewater sample, an increased amount of Na-Z (L/S =10 $cm^3 \cdot g^{-1}$) was used. The increased amount of the adsorbent in the system would increase the available surface of the adsorbent and the number of active sites, enabling the more efficient removal of various metal ions from wastewater.

3.3. Removal of metal ions from wastewater

Adsorption test results for wastewater treatment are expressed in terms of the adsorption capacity (*qt*) and the efficiency of the process in removing certain metal ions over time and presented in Figure 8. The *qt* and the efficiency of the adsorption process show the same trend over time, so they are shown on the same graph as the primary and secondary y-axis, respectively.

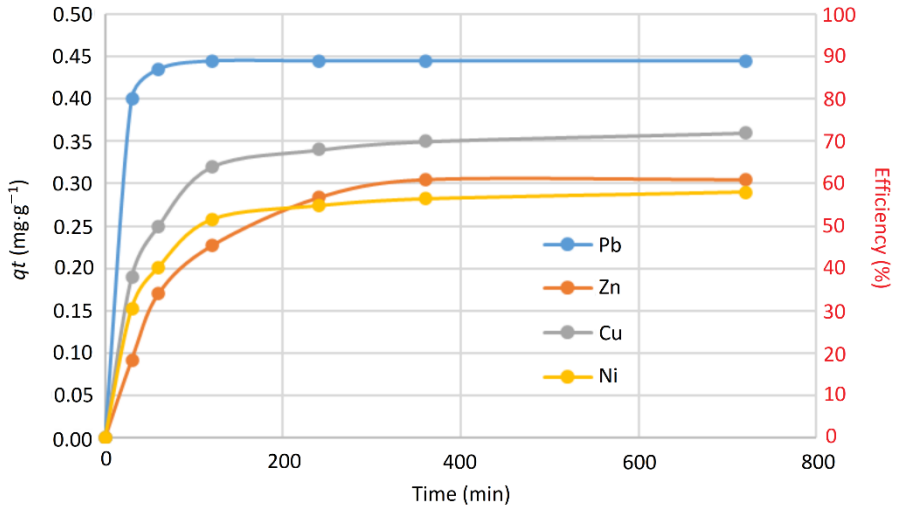

Figure 8. *The amount of metal ions adsorbed and efficiency of metals ion removal over time for wastewater treatment process*

Figure 8 shows that adsorption of metal ions (*qt*) is reduced in the adsorption test of the multi-component wastewater sample compared to individual metal ion adsorption tests due to

the increased amount of adsorbent (L/S 10 $cm^3 \cdot g^{-1}$). The highest *qt* is reached for Pb^{2+} (0.45 $mg \cdot g^{-1}$), then for Cu^{2+} (0.36 $mg \cdot g^{-1}$) and Zn^{2+} (0.31 $mg \cdot g^{-1}$), and the least for Ni^{2+} (0.29 $mg \cdot g^{-1}$). Consequently, removal efficiency follows this order Pb^{2+} (89%) > Cu^{2+} (72%) > Zn^{2+} (61%) >Ni^{2+} (58%). Most documented studies confirm that zeolite adsorbent has a higher selectivity towards Pb^{2+} and Cu^{2+} ions, while the adsorption capacity of Zn^{2+} and Ni^{2+} decreases significantly in the presence of other cations [27] . Several factors influence the selectivity of zeolites towards ions such as the ionic radii, hydrated ionic radii, and free energy of hydration [9]. In the aqueous solution, the metal ions will be present in their hydrated forms, so the smaller hydrated ionic radii will enable their easier transfer through the pores of the adsorbent. Also, the low hydration energy will allow the ion to more easily lose water molecules and bind to the active sites. These characteristics of investigated metal ions are listed in Table 4.

Table 4. *Hydrated ionic radii and free energy of hydration of Pb^{2+}, Zn^{2+}, Cu^{2+} and Ni^{2+} ions*

Characteristic	Pb^{2+}	Zn^{2+}	Cu^{2+}	Ni^{2+}
Hydrated ionic radii (Å) [28]	4.01	4.30	4.19	4.04
Free energy of hydration ($kJ \cdot mol^{-1}$) [12]	-1480	-2044	-2100	-2106

The Pb^{2+} ion has the smallest hydrated radii (4.01Å) and the lowest hydration energy (-1425 $kJ \cdot mol^{-1}$) compared to the other investigated ions and is most easily adsorbed using Na-enriched natural zeolite. These characteristics also resulted in the Pb^{2+} ion having the highest PFO adsorption rate of 0.09 $mg \cdot g^{-1} \cdot min^{-1}$ (external and internal diffusion mechanism) and PSO adsorption rate of 0.32 $mg \cdot g^{-1} \cdot min^{-1}$ (binding to active sites) at the beginning of adsorption process, as shown in Figure 6. Other works confirmed zeolite's highest affinity toward Pb^{2+} ion [9-13, 26, 29]. Cu^{2+} and Ni^{2+} have similar characteristics of hydrated radii and hydration energy, Table 4. However, the rate of adsorption on active sites (PSO rate), as the rapid kinetic of the Cu^{2+} and Ni^{2+} adsorption processes, is higher for Cu^{2+} (0.28 $mg \cdot g^{-1} \cdot min^{-1}$) than for Ni^{2+} ions (0.11 $mg \cdot g^{-1} \cdot min^{-1}$), Figure 7. This result is then reflected in the significantly higher adsorption capacity/removal efficiency of Cu^{2+} than that of Ni^{2+}, Figure 8. The research by Merrikhpour and Jalali (2012) [30] found that Ni^{2+} retention by zeolite is the result of the ion exchange reaction, while the retention of Pb^{2+} and Cu^{2+} is the result of both ion exchange and precipitation. Majdan et al. (2003) [31] confirmed that Cu^{2+} forms a new phase under acidic conditions during the adsorption process on the zeolite and therefore its affinity to the zeolite is very high in contrast to Ni^{2+}. Hong et al. (2019) [32] discovered that hierarchical pore geometry of zeolite has great influence on the adsorption of Ni^{2+}, and that using a zeolite with larger micro and mesopores exhibits significantly increased Ni^{2+} adsorption amount. This is in agreement with the adsorption rate results shown in Figure 7 where it can be seen that external/internal ion diffusion, as the slower process, is the rate limiting mechanism for Ni^{2+} adsorption. The radius of the hydrated Zn^{2+} ion (4.30 Å) is the largest one compared to the other investigated ions, Table 4. Oren and Kaya (2006) [33] explained that lower adsorption rates of Zn^{2+} on zeolites might be due to the difficulty in the penetration of hydrated Zn^{2+} ions into the zeolite channels. On the other hand, its PFO adsorption rate of 0.030 $mg \cdot g^{-1} \cdot min^{-1}$ (Figure 6) is higher than the PFO rates of Cu^{2+} (0.010 $mg \cdot g^{-1} \cdot min^{-1}$) and Ni^{2+} (0.013 $mg \cdot g^{-1} \cdot min^{-1}$) (Figure 7). Also, its lower hydration free energy (-2044 $kJ \cdot mol^{-1}$) should result in a higher PSO rate, which is not the case. The rate of adsorption of Zn^{2+} ions to active sites (0.029 $mg \cdot g^{-1} \cdot min^{-1}$) is the lowest one among the investigated ions. This confirms that the Zn^{2+} adsorption process on zeolite is a complex process that requires further investigations. Li et al. (2019) demonstrated that some cation sites on zeolites can only be exchanged by selective alien cations with specific favorable characteristics in terms of size, charge, radius of hydrated ions and hydration energy [11]. The selectivity of zeolite was probably caused by its propinquity to the other metal ions

in the solution [27]. Due to low PFO and PSO adsorption rates, the equilibrium of the Zn^{2+} removal process was reached much later in the adsorption tests of individual metal ions (L/S 100 $cm^3 \cdot g^{-1}$). However, increasing the amount of Na-Z in the wastewater treatment test (L/S 10 $cm^3 \cdot g^{-1}$) enabled a decrease in the time to reach equilibrium below 400 min and to achieve the Zn^{2+} ion removal efficiency of 61%, Figure 8.

4. Conclusion

The characteristics of Na-enriched zeolite as an adsorbent can be attributed to its main mineral phase clinoptilolite. With a specific surface area of 41 $m^2 g^{-1}$ and a cation exchange capacity of 176 mmol M^+ per 100 g of Na-Z, the adsorbent has good potential for removing Pb^{2+}, Zn^{2+}, Cu^{2+} and Ni^{2+} ions from wastewater.

Weber-Morris model results indicate that the adsorption of Pb^{2+}, Zn^{2+}, Cu^{2+} and Ni^{2+} using Na-Z is a complex process and that intraparticle diffusion is not the sole rate-limiting step in the adsorption mechanism. Investigation of the adsorption kinetics of individual metal ions by applying the PFO, PSO and MO kinetic models showed that all three models have good results in fitting the experimental data. The results of these kinetic models confirm that adsorption processes of metal ions are dominated by multiple rate-limiting steps. Such complex processes are best defined by the more general MO model. For the adsorption of Pb^{2+} ions, both mechanisms of ion diffusion and adsorption to active sites could be rate-limiting steps. The mechanism of ion diffusion occurs more rapidly than adsorption to active sites in the Zn^{2+} ions adsorption process, indicating that adsorption on active sites is the rate-limiting mechanism. In the case of the Cu^{2+} and Ni^{2+} ions adsorption , diffusion of ions is the rate limiting step. Within the MO model, the PFO rate (external/internal diffusion) and the PSO rate (adsorption on the active sites) were calculated, which enabled to predict and explain the results of the metal ion removal process from a multicomponent wastewater sample by adsorption on Na-Z.

In wastewater treatment, Na-enriched natural zeolite showed the highest selectivity towards Pb^{2+} ions (89% removal efficiency). Also, Pb^{2+} ions have the highest rates of diffusion (PSO rate) and binding to active sites (PSO rate), which is associated with the small radius of the hydrated Pb^{2+} ion and its low hydration energy. Although Cu^{2+} and Ni^{2+} ions have similar values of hydrated ion radius and hydration energy, the higher PSO rate of Cu^{2+} ions reflected higher removal efficiency compared to Ni^{2+} ions, 72% and 58%, respectively. In the process of removing Zn^{2+} ions from wastewater, the adsorption equilibrium and removal efficiency of 61% was reached much later compared to the other investigated ions due to the low rate of adsorption to active sites. Achieved adsorption capacities of metal ions on Na-enriched natural zeolite in wastewater treatment are Pb^{2+} (0.45 $mg \cdot g^{-1}$) > Cu^{2+} (0.36 $mg \cdot g^{-1}$) > Zn^{2+} (0.31 $mg \cdot g^{-1}$) > Ni^{2+} (0.29 $mg \cdot g^{-1}$) at L/S ratio of 10 $cm^3 \cdot g^{-1}$.

The presented results of the adsorption kinetics tests, and then their application in the removal of metal ions from the synthetic multicomponent wastewater sample, showed that Na-enriched natural zeolite can be used as an effective adsorbent in wastewater treatment.

Acknowledgements:

This work has been financially supported by grants issued from the Ministry of Science, Technological Development and Innovation of the Republic of Serbia (Contract No. 451-03-47/2023-01/200287, 451-03-47/2023-01/200135 and 451-03-47/2023-01/200288).

References

1. Brinkmann, T., et al., *Best available techniques (BAT) reference document for common waste water and waste gas treatment/management systems in the chemical sector.* Publications Office of the European Union, 2016: p. 3.
2. Crini, G., et al., *Conventional and non-conventional adsorbents for wastewater treatment.* Environmental Chemistry Letters, 2019. **17**: p. 195-213.
3. El-Sayed, M.E., *Nanoadsorbents for water and wastewater remediation.* Science of the Total Environment, 2020. **739**: p. 139903.
4. Bessa, R.A., et al., *Hierarchical zeolite based on multiporous zeolite A and bacterial cellulose: An efficient adsorbent of Pb2+*. Microporous and Mesoporous Materials, 2021. **312**: p. 110752.
5. Safie, N. and A. Zahrim, *Recovery of nutrients from sewage using zeolite-chitosan-biochar adsorbent: current practices and perspectives.* Journal of Water Process Engineering, 2021. **40**: p. 101845.
6. Jia, X., C. Jo, and A.C. Yip, *Synthesis strategies for hierarchical zeolites.* Heterogeneous catalysts: advanced design, characterization and applications, 2021. **1**: p. 119-145.
7. Koohsaryan, E. and M. Anbia, *Nanosized and hierarchical zeolites: A short review.* Chinese Journal of Catalysis, 2016. **37**(4): p. 447-467.
8. Obaid, S.S., et al., *Heavy metal ions removal from waste water bythe natural zeolites.* Materials Today: Proceedings, 2018. **5**(9): p. 17930-17934.
9. de Magalhães, L.F., G.R. da Silva, and A.E.C. Peres, *Zeolite application in wastewater treatment.* Adsorption Science & Technology, 2022. **2022**: p. 1-26.
10. Velarde, L., et al., *Adsorption of heavy metals on natural zeolites: A review.* Chemosphere, 2023: p. 138508.
11. Li, Y., et al., *Removal of Zn2+, Pb2+, Cd2+, and Cu2+ from aqueous solution by synthetic clinoptilolite.* Microporous and Mesoporous Materials, 2019. **273**: p. 203-211.
12. Mihaly-Cozmuta, L., et al., *Adsorption of heavy metal cations by Na-clinoptilolite: Equilibrium and selectivity studies.* Journal of environmental management, 2014. **137**: p. 69-80.
13. Wang, S. and Y. Peng, *Natural zeolites as effective adsorbents in water and wastewater treatment.* Chemical engineering journal, 2010. **156**(1): p. 11-24.
14. Wang, J. and X. Guo, *Adsorption kinetic models: Physical meanings, applications, and solving methods.* Journal of Hazardous materials, 2020. **390**: p. 122156.
15. Obradović, B., *Guidelines for general adsorption kinetics modeling.* Hemijska industrija, 2020. **74**(1): p. 65-70.
16. Yuna, Z., *Review of the natural, modified, and synthetic zeolites for heavy metals removal from wastewater.* Environmental Engineering Science, 2016. **33**(7): p. 443-454.
17. Lima, E.C., et al., *Is one performing the treatment data of adsorption kinetics correctly?* Journal of Environmental Chemical Engineering, 2021. **9**(2): p. 104813.
18. Guo, X. and J. Wang, *A general kinetic model for adsorption: Theoretical analysis and modeling.* Journal of Molecular Liquids, 2019. **288**: p. 111100.
19. Narváez, L., et al., *Electrochemical stability of steel reinforced bars embedded in cement mortars containing clinoptilolite as supplementary.* International Journal of Electrochemical Science, 2015. **10**(12): p. 10003-10016.
20. Jevtić, S., et al., *The iron (III)-modified natural zeolitic tuff as an adsorbent and carrier for selenium oxyanions.* Microporous and mesoporous materials, 2014. **197**: p. 92-100.
21. Lian, Q., et al., *Enhanced Pb (II) adsorption onto functionalized ordered mesoporous carbon (OMC) from aqueous solutions: the important role of surface property and*

adsorption mechanism. Environmental Science and Pollution Research, 2020. **27**: p. 23616-23630.
22. Jain, S.N., et al., *Nonlinear regression approach for acid dye remediation using activated adsorbent: Kinetic, isotherm, thermodynamic and reusability studies.* Microchemical Journal, 2019. **148**: p. 605-615.
23. Taguba, M.A.M., et al., *Nonlinear isotherm and kinetic modeling of Cu (II) and Pb (II) uptake from water by MnFe2O4/chitosan nanoadsorbents.* Water, 2021. **13**(12): p. 1662.
24. Danalıoğlu, S.T., et al., *Chitosan grafted SiO 2–Fe 3 O 4 nanoparticles for removal of antibiotics from water.* Environmental Science and Pollution Research, 2018. **25**: p. 36661-36670.
25. Stojakovic, D., et al., *A study of the removal of copper ions from aqueous solution using clinoptilolite from Serbia.* Clays and Clay Minerals, 2011. **59**(3): p. 277-285.
26. Khan, S., M. Idrees, and M. Bilal, *Revealing and elucidating chemical speciation mechanisms for lead and nickel adsorption on zeolite in aqueous solutions.* Colloids and Surfaces A: Physicochemical and Engineering Aspects, 2021. **623**: p. 126711.
27. Malamis, S. and E. Katsou, *A review on zinc and nickel adsorption on natural and modified zeolite, bentonite and vermiculite: Examination of process parameters, kinetics and isotherms.* Journal of hazardous materials, 2013. **252**: p. 428-461.
28. Nightingale Jr, E., *Phenomenological theory of ion solvation. Effective radii of hydrated ions.* The Journal of Physical Chemistry, 1959. **63**(9): p. 1381-1387.
29. Budianta, W. *Laboratory study on the use of natural zeolite from Gunungkidul, Indonesia for Cu, Pb, Zn and Cd immobilization in soil*. in *E3S Web of Conferences*. 2020. EDP Sciences.
30. Merrikhpour, H. and M. Jalali, *Comparative and competitive adsorption of cadmium, copper, nickel, and lead ions by Iranian natural zeolite.* Clean Technologies and Environmental Policy, 2013. **15**: p. 303-316.
31. Majdan, M., et al., *Equilibrium study of selected divalent d-electron metals adsorption on A-type zeolite.* Journal of colloid and interface science, 2003. **262**(2): p. 321-330.
32. Hong, M., et al., *Heavy metal adsorption with zeolites: The role of hierarchical pore architecture.* Chemical Engineering Journal, 2019. **359**: p. 363-372.
33. Ören, A.H. and A. Kaya, *Factors affecting adsorption characteristics of Zn2+ on two natural zeolites.* Journal of hazardous materials, 2006. **131**(1-3): p. 59-65.